Acta Crystallographica Section F
Structural Biology and Crystallization Communications
ISSN 1744-3091

Crystallization and preliminary X-ray analysis of the reductase component of *p*-hydroxyphenylacetate 3-hydroxylase from *Acinetobacter baumannii*

Worrapoj Oonanant,[a] Jeerus Sucharitakul,[b] Pimchai Chaiyen[a] and Jirundon Yuvaniyama[a]*

[a]Department of Biochemistry and Center for Excellence in Protein Structure and Function, Faculty of Science, Mahidol University, Rama 6 Road, Phayathai, Bangkok 10400, Thailand, and [b]Department of Biochemistry, Faculty of Dentistry, Chulalongkorn University, Henri-Dunant Road, Patumwan, Bangkok 10330, Thailand

Correspondence e-mail: scjyv@mahidol.ac.th

Received 21 February 2012
Accepted 17 April 2012

p-Hydroxyphenylacetate 3-hydroxylase (HPAH) from *Acinetobacter baumannii* catalyzes the hydroxylation of *p*-hydroxyphenylacetate (HPA) at the *ortho* position to yield 3,4-dihydroxyphenylacetate (DHPA). HPAH from *A. baumannii* is a two-component flavoprotein consisting of a smaller reductase (C_1) component and a larger oxygenase (C_2) component. The C_1 component supplies a reduced flavin in its free form to the C_2 counterpart for hydroxylation. In addition, HPA can bind to C_1 and enhance the flavin-reduction rate without becoming hydroxylated. The recombinant C_1 component was purified and crystallized using the microbatch method at 295 K. X-ray diffraction data were collected to 2.3 Å resolution using synchrotron radiation on the BL13B1 beamline at NSRRC, Taiwan. The crystal belonged to the orthorhombic space group $P2_12_12_1$, with unit-cell parameters a = 47.78, b = 59.92, c = 211.85 Å, and contained two molecules of C_1 per asymmetric unit.

1. Introduction

p-Hydroxyphenylacetate 3-hydroxylase (HPAH; EC 1.14.13.3) is a two-component flavoprotein that catalyzes the hydroxylation of *p*-hydroxyphenylacetate (HPA) to form 3,4-dihydroxyphenylacetate (DHPA). HPAH has been identified and studied in the bacteria *Pseudomonas putida* (Arunachalam *et al.*, 1992, 1994), *Escherichia coli* W (Galán *et al.*, 2000), *Acinetobacter baumannii* (Chaiyen *et al.*, 2001) and *Pseudomonas aeruginosa* (Chakraborty *et al.*, 2010), as well as in the archaea *Sulfolobus tokodaii* strain 7 (Okai *et al.*, 2006) and *Thermus thermophilus* HB8 (Kim *et al.*, 2008). HPAH comprises a smaller reductase and a larger oxygenase on separate polypeptide chains. The reductase functions to generate a reduced flavin, which is able to diffuse to the oxygenase component for the hydroxylation reaction without a requirement for protein–protein interaction (Sucharitakul *et al.*, 2005, 2006, 2007). The dihydroxylated product DHPA is ultimately converted to intermediate metabolites in the TCA cycle (Sparnins *et al.*, 1974). Therefore, the enzyme is important for the bacterial biodegradation of lignin and phenolic compounds. Additional biological functions of HPAH in *A. baumannii* (which is an opportunistic pathogen) may also exist and are currently being investigated by our group.

HPAH from *A. baumannii* has been isolated and extensively investigated (Chaiyen *et al.*, 2001; Thotsaporn *et al.*, 2004, 2011; Sucharitakul *et al.*, 2005, 2006, 2007; Ruangcharn *et al.*, 2011; Tongsook *et al.*, 2011). The enzyme possesses interesting properties which differ from those of other previously studied HPAH systems. The reductase component (C_1) of *A. baumannii* was purified with a tightly bound FMN molecule in each subunit. The enzyme is a homodimer with a subunit mass of about 35 kDa, which is similar to that of the reductase component of *P. putida* HPAH but larger than that of *E. coli* W HPAH. Its function is to generate reduced FMN for HPA hydroxylation by the larger oxygenase component (C_2). Studies of its kinetic mechanism have revealed that C_1 is also able to bind HPA without catalyzing its hydroxylation (Sucharitakul *et al.*, 2005). Such HPA binding enhances the rates of both the reduction of FMN and the release of reduced FMN from C_1 (Sucharitakul *et al.*, 2005, 2007). This effect has not been observed for any of the known flavin

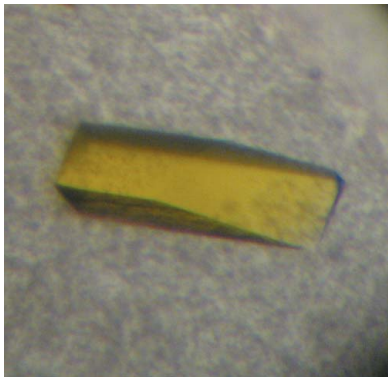

reductases from various organisms apart from the reductase component of *P. putida* HPAH (Arunachalam *et al.*, 1992, 1994) and component B of nitrilotriacetate (NTA) monooxygenase from *Chelatobacter* strain ATCC 29600 (Uetz *et al.*, 1992). Sequence analysis also revealed that the N-terminal half of C_1 is similar to the flavin-binding domains of other reductases (Thotsaporn *et al.*, 2004). In contrast, its C-terminal half, which is absent in the other reductases, is similar to the corresponding sequences of the reductase components of *Chelatobacter* NTA monooxygenase and *P. putida* HPAH (13 and 47% identity over 144 amino acids, respectively). Therefore, these C-terminal sequences may be involved in HPA binding and may be responsible for substrate stimulation in the reaction.

The crystal structures of flavin reductases from various organisms have been determined, including phenol 2-hydroxylase (PheA2) from *Bacillus thermoglucosidasius* A7 (PDB entry 1rz0; van den Heuvel *et al.*, 2004), HpaC of HPAH from *S. tokodaii* strain 7 (PDB entry 2d36; Okai *et al.*, 2006) and HpaC from *T. thermophilus* HB8 (PDB entry 2ecr; Kim *et al.*, 2008). All of these structures share the same protein fold and lack the extra C-terminal domain found in C_1. Recently, the structure of NTA monooxygenase component B from *Mycobacterium thermoresistibile* (PDB entry 3nfw; Zhang *et al.*, 2011) has been determined. This enzyme possesses a similar but much smaller C-terminal extension that is expected to regulate its function, as in C_1. At around 130 residues shorter in its C-terminal sequence in comparison with C_1, the C-terminal structure of this enzyme is likely to differ significantly from those of C_1 and the reductases of *P. putida* HPAH and *Chelatobacter* NTA monooxygenase. Aiming to use C_1 from *A. baumannii* HPAH as a representative structure of this group of reductases, we present its crystallization and preliminary X-ray analysis.

2. Materials and methods

2.1. Expression and purification

Recombinant C_1 was overexpressed and purified as previously reported (Chaiyen *et al.*, 2001; Thotsaporn *et al.*, 2004) with the following modifications. Briefly, cells were grown in Luria–Bertani medium supplemented with 100 µg ml^{-1} ampicillin at 310 K until the OD_{600} reached 1.0–1.5. Protein expression was induced with 1 m*M* isopropyl *β*-D-1-thiogalactopyranoside at 289 K. The cells were harvested after 8 h of induction or when the OD_{600} reached 4.0 by centrifugation at 5500*g* for 10 min at 277 K. The cell paste was resuspended in a lysis buffer consisting of 100 m*M* sodium phosphate pH 8.0, 5 m*M* ethylenediaminetetraacetic acid (EDTA), 5 m*M* dithiothreitol (DTT), 60 µ*M* phenylmethylsulfonyl fluoride. The cell suspension was disrupted on ice by ultrasonication and the lysate was centrifuged at 3500*g* for 1 h at 277 K. All subsequent purification steps were performed at 277 K. The supernatant was precipitated by 40–80% ammonium sulfate fractionation. The yellow pellet was resuspended and concentrated in buffer *A* (10 m*M* sodium phosphate buffer pH 7.0, 0.5 m*M* EDTA, 1 m*M* DTT). The concentrated enzyme was centrifuged at 3500*g* for 10 min before applying it onto a DEAE-Sepharose Fast Flow column (GE Healthcare) that had been pre-equilibrated and was subsequently washed with the same buffer. The enzyme was eluted with a gradient of 0–250 m*M* NaCl in buffer *A*. The enzyme fractions were pooled based on the OD_{458} and then precipitated by 80% ammonium sulfate saturation. The yellow pellet was dissolved in a minimal volume of 15% saturated ammonium sulfate in buffer *A*. The dissolved enzyme solution was centrifuged at 3500*g* for 10 min and loaded onto a Phenyl-Sepharose column (GE Healthcare) that had been pre-equilibrated and was subsequently washed with 15% saturated ammonium sulfate in buffer *A*. The enzyme was eluted with a gradient of 15–0% ammonium sulfate and 0–40%(*v*/*v*) ethylene glycol in buffer *A*. Fractions containing C_1 were pooled based on the OD_{458}/OD_{280} ratio. The purity of the enzyme was judged by 12.5% SDS–PAGE. The C_1 pool was concentrated using Amicon Ultra-4 centrifugal filter units with 10 kDa molecular-weight cutoff (Millipore) and was loaded onto a G-25 column for buffer exchange to 50 m*M* MOPS pH 7.0, 0.3 m*M* EDTA, 1 m*M* DTT. It was then concentrated to 10 mg ml^{-1} based on its known extinction coefficient at 458 nm of 12 800 M^{-1} cm^{-1} (Sucharitakul *et al.*, 2005). HPA (10 m*M* in 50 m*M* MOPS pH 7.0) was added to an aliquot of the concentrated C_1 to give a final concentration of 1 m*M* for subsequent crystallization experiments.

Table 1
Data-collection and processing statistics.

Values in parentheses are for the highest resolution shell.

X-ray source	Beamline BL13B1, NSRRC
Wavelength (Å)	1.0000
Resolution (Å)	50.00–2.30 (2.38–2.30)
Space group	$P2_12_12_1$
Unit-cell parameters (Å)	a = 47.78, b = 59.92, c = 211.85
Total reflections	143944
Unique reflections	27013 (2261)
Completeness (%)	95.7 (81.6)
Multiplicity	5.3 (3.1)
$\langle I/\sigma(I)\rangle$	40.3 (17.1)
$R_{\rm merge}$†	0.035 (0.064)

† $R_{\rm merge} = \sum_{hkl}\sum_i |I_i(hkl) - \langle I(hkl)\rangle| / \sum_{hkl}\sum_i I_i(hkl)$, where $I_i(hkl)$ is the intensity of the *i*th measurement of an equivalent reflection with indices *hkl*.

2.2. Crystallization

The purified C_1 was freshly prepared and filtered through 0.22 µm Amicon Ultrafree-MC centrifugal filter devices (Millipore) prior to crystallization setup. Crystallization of C_1 was carried out using the microbatch method (Chayen *et al.*, 1992; D'Arcy *et al.*, 2004) in 60-well Mini Tray plates (Nunc) at 295 K. A droplet was set up under oil (Babi Mild Natural N'Mild baby oil; Chitnumsub *et al.*, 2004) by mixing equal volumes (1–3 µl) of protein and crystallization solutions. Yellow single crystals were obtained using 20%(*m*/*v*) PEG 400, 0.1 *M* sodium acetate pH 4.6 as a precipitant. After optimization by varying the concentration of PEG 400 and glycerol, crystals were produced in a clear droplet from conditions consisting of 20–25%(*m*/*v*) PEG 400, 0.1 *M* sodium acetate pH 4.6, 10%(*v*/*v*) glycerol within 1 d and reached approximate dimensions of 0.15 × 0.15 × 0.3 mm in 3 d.

2.3. X-ray data collection

The crystals were quickly dipped in Paratone-N as a cryoprotectant before vitrification and data collection. Initial X-ray diffraction experiments were performed at the Center for Excellence in Protein Structure and Function, Faculty of Science, Mahidol University, Thailand. The crystals were mounted on a nylon cryoloop (0.2–0.3 mm) and exposed to X-ray radiation using an in-house rotating-anode X-ray generator (Rigaku RU-H3R; Cu $K\alpha$; λ = 1.5418 Å) operating at 50 kV and 100 mA with an R-AXIS IV^{++} detector system (Rigaku/MSC) for preliminary diffraction analysis. X-ray diffraction data were collected using an ADSC Quantum-315 CCD detector under a nitrogen cryostream (100 K) on beamline BL13B1 at the National Synchrotron Radiation Research Center (NSRRC), Taiwan. The crystal-to-detector distance and the offset of the detector position in the vertical direction were optimized to 400 and 25 mm, respectively, in order to collect X-ray reflections at higher resolution

since the crystal was able to diffract beyond 2.6 Å resolution. A total of 360 frames with 0.5° oscillation width and 5 s exposure time per frame were collected and processed to 2.3 Å resolution. Data were processed using the *CrystalClear* program suite (Pflugrath, 1999) and the *HKL*-2000 package (Otwinowski & Minor, 1997) for the in-house and synchrotron data sets, respectively. X-ray data-collection statistics for the synchrotron data set are summarized in Table 1.

3. Results and discussion

The recombinant C_1 component of *A. baumannii* HPAH was overexpressed in *E. coli* and purified to >95% homogeneity as judged by SDS–PAGE and native PAGE. The method produced approximately 150 mg pure protein from 3.6 l cell culture. The purified C_1 was crystallized using the microbatch method. Single rod-shaped crystals suitable for X-ray data collection were reproducibly obtained (Fig. 1). Their yellow colour indicated the presence of oxidized flavin molecules in the crystals. The crystals diffracted X-rays to beyond 2.6 Å resolution using our home-source X-ray equipment. Data processing showed that this crystal form belonged to the orthorhombic space group $P2_12_12_1$, with a long unit-cell length in the *c* dimension. Overlapping reflections were observed, which limited the usable data to only low resolution, despite the fact that the crystals diffracted much further. To overcome this problem, the orientation of the crystal was optimized by aligning its *c* axis parallel to the spindle angle of the goniometer. Practically, this was very difficult as the *c* axis was along one of the widths of the thin rod-shaped crystals, while the viscous cryoprotectant tended to pull the crystal back along the oval-shaped nylon cryoloop in its typical geometry parallel to the pin. Moreover, prolonged soaking (>10 s) in the cryoprotectant caused a dramatic decrease in diffraction, limiting the time that could be used for crystal orientation. Therefore, an L-shaped nylon cryoloop was made to speed up the mounting process, which allowed successful vitrification of a crystal in the desired orientation with high-quality X-ray diffraction (Fig. 2). In addition to the optimization of data collection by crystal orientation, the detector was also offset to maximize the collection of higher angle diffraction. A complete data set was collected to 2.3 Å resolution using synchrotron radiation. The data were processed in the orthorhombic space group $P2_12_12_1$, with unit-cell parameters $a = 47.78$, $b = 59.92$, $c = 211.85$ Å. The calculated molecular volume (Matthews coefficient; Matthews, 1968) of 2.14 Å^3 Da^{-1} and solvent content of 42.7% suggested that there were two molecules of C_1 in the asymmetric unit.

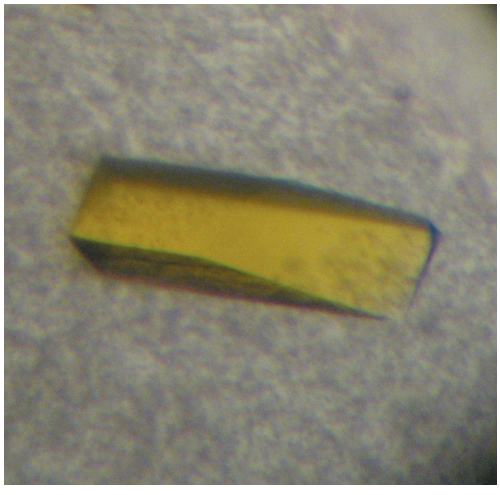

Figure 1
A crystal of the C_1 component of *A. baumannii* HPAH. This orthorhombic crystal grew to dimensions of 0.15 × 0.15 × 0.5 mm in 3 d.

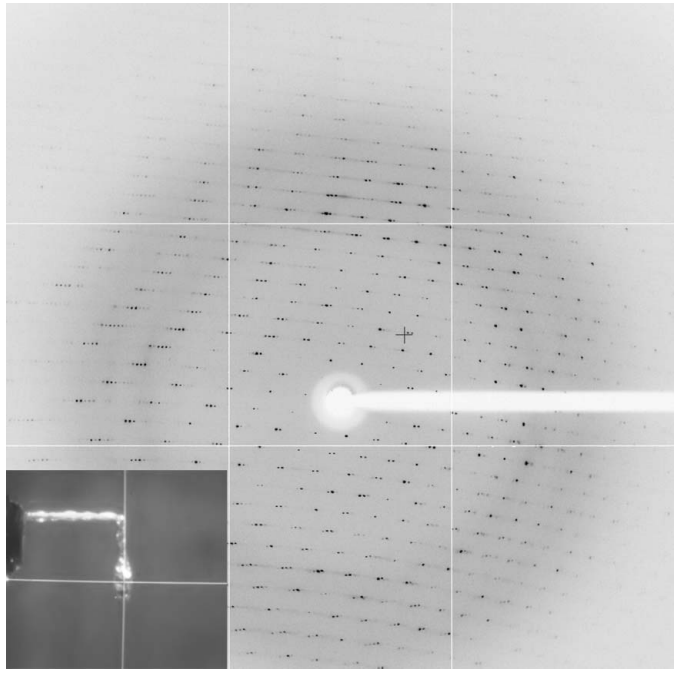

Figure 2
X-ray diffraction pattern of the C_1 crystal. The crystal was mounted such that its long axis was nearly parallel to the spindle axis to minimize reflection overlap. This was accomplished by the use of an L-shaped nylon loop (inset). While maintaining the crystal-to-detector distance of 400 mm to prevent spot overlaps, the CCD detector was offset to allow the collection of higher resolution data at the upper side of the detector.

The self-rotation function calculated in *AMoRe* (Navaza, 1994; Winn *et al.*, 2011) showed a significant peak (62.3% of the self-peak) representing a twofold rotation axis located around 13° from the *c* axis, while no outstanding peak was found in the native Patterson. This suggested a dimeric structure for C_1, which is consistent with the previously reported results of gel-filtration chromatography (Chaiyen *et al.*, 2001). We attempted to determine the structure of C_1 using the molecular-replacement method. The coordinates of the PheA2 component of phenol hydroxylase from *B. thermoglucosidasius* A7 (PDB entry 1rz0; 37% sequence identity over 161 residues) was used as a template to construct search models using either all atoms or polyalanines and conserved residues. However, no reasonable solution could be obtained using either monomeric or dimeric structures of PheA2. Since the PheA2 templates would account for only 25–50% of the molecular size of the dimeric C_1 in the asymmetric unit, they may be too small to provide sufficient phases for C_1 structure determination. In addition, monomeric or dimeric structures of NTA monooxygenase component B from *M. thermoresistibile* (PDB entry 3nfw; 29% sequence identity over 210 residues) were similarly used as search templates with a lack of success. This may suggest that the structure of the short C-terminal extension of 3nfw differs significantly from that of C_1. Hence, other phasing methods such as MIR or MAD are required for phase determination of the C_1 structure.

This work was supported by the Synchrotron Light Research Institute, Thailand (grant 2-2549/LS02 to JY), The Thailand Research Fund (grant BRG5480001 to PC) and the Faculty of Science, Mahidol

University (to PC). We acknowledge the provision of beamtime and staff support at beamline BL13B1, NSRRC, Taiwan.

References

Arunachalam, U., Massey, V. & Miller, S. M. (1994). *J. Biol. Chem.* **269**, 150–155.

Arunachalam, U., Massey, V. & Vaidyanathan, C. S. (1992). *J. Biol. Chem.* **267**, 25848–25855.

Chaiyen, P., Suadee, C. & Wilairat, P. (2001). *Eur. J. Biochem.* **268**, 5550–5561.

Chakraborty, S., Ortiz-Maldonado, M., Entsch, B. & Ballou, D. P. (2010). *Biochemistry*, **49**, 372–385.

Chayen, N. E., Shaw Stewart, P. D. & Blow, D. M. (1992). *J. Cryst. Growth*, **122**, 176–180.

Chitnumsub, P., Yavaniyama, J., Vanichtanankul, J., Kamchonwongpaisan, S., Walkinshaw, M. D. & Yuthavong, Y. (2004). *Acta Cryst.* D**60**, 780–783.

D'Arcy, A., Sweeney, A. M. & Haber, A. (2004). *Methods*, **34**, 323–328.

Galán, B., Díaz, E., Prieto, M. A. & García, J. L. (2000). *J. Bacteriol.* **182**, 627–636.

Heuvel, R. H. van den, Westphal, A. H., Heck, A. J., Walsh, M. A., Rovida, S., van Berkel, W. J. & Mattevi, A. (2004). *J. Biol. Chem.* **279**, 12860–12867.

Kim, S.-H., Hisano, T., Iwasaki, W., Ebihara, A. & Miki, K. (2008). *Proteins*, **70**, 718–730.

Matthews, B. W. (1968). *J. Mol. Biol.* **33**, 491–497.

Navaza, J. (1994). *Acta Cryst.* A**50**, 157–163.

Okai, M., Kudo, N., Lee, W. C., Kamo, M., Nagata, K. & Tanokura, M. (2006). *Biochemistry*, **45**, 5103–5110.

Otwinowski, Z. & Minor, W. (1997). *Methods Enzymol.* **276**, 307–326.

Pflugrath, J. W. (1999). *Acta Cryst.* D**55**, 1718–1725.

Ruangchan, N., Tongsook, C., Sucharitakul, J. & Chaiyen, P. (2011). *J. Biol. Chem.* **286**, 223–233.

Sparnins, V. L., Chapman, P. J. & Dagley, S. (1974). *J. Bacteriol.* **120**, 159–167.

Sucharitakul, J., Chaiyen, P., Entsch, B. & Ballou, D. P. (2005). *Biochemistry*, **44**, 10434–10442.

Sucharitakul, J., Chaiyen, P., Entsch, B. & Ballou, D. P. (2006). *J. Biol. Chem.* **281**, 17044–17053.

Sucharitakul, J., Phongsak, T., Entsch, B., Svasti, J., Chaiyen, P. & Ballou, D. P. (2007). *Biochemistry*, **46**, 8611–8623.

Thotsaporn, K., Chenprakhon, P., Sucharitakul, J., Mattevi, A. & Chaiyen, P. (2011). *J. Biol. Chem.* **286**, 28170–28180.

Thotsaporn, K., Sucharitakul, J., Wongratana, J., Suadee, C. & Chaiyen, P. (2004). *Biochim. Biophys. Acta*, **1680**, 60–66.

Tongsook, C., Sucharitakul, J., Thotsaporn, K. & Chaiyen, P. (2011). *J. Biol. Chem.* **286**, 44491–44502.

Uetz, T., Schneider, R., Snozzi, M. & Egli, T. (1992). *J. Bacteriol.* **174**, 1179–1188.

Winn, M. D. *et al.* (2011). *Acta Cryst.* D**67**, 235–242.

Zhang, Y., Edwards, T. E., Begley, D. W., Abramov, A., Thompkins, K. B., Ferrell, M., Guo, W. J., Phan, I., Olsen, C., Napuli, A., Sankaran, B., Stacy, R., Van Voorhis, W. C., Stewart, L. J. & Myler, P. J. (2011). *Acta Cryst.* F**67**, 1100–1105.